THE JOURNAL OF PHYSICAL CHEMISTRY B

Article

pubs.acs.org/JPCB

Nonstraight Nanochannels Transfer Water Faster Than Straight Nanochannels

T. Qiu,[†] X. W. Meng,[‡] and J. P. Huang*,[†]

[†]Department of Physics and State Key Laboratory of Surface Physics, Fudan University, Shanghai 200433, China

[‡]College of Sciences, China University of Mining and Technology, Xuzhou 221116, China

ABSTRACT: Understanding the flow of liquids and particularly water in nanochannels is important for scientific and technological applications, such as for filtration and drug delivery. Here we perform molecular dynamics simulations to investigate the transfer of single-file water molecules across straight or nonstraight single-walled carbon nanotubes (SWCNTs). In contrast with the macroscopic scenario, the nonstraight nanostructure can increase the water permeation. Remarkably, compared with the straight SWCNT, the nonstraight SWCNT with the minimal bending angle of 35° in the simulations can enhance the water transport up to 3.5 times. This enhancement mainly originates from the Lennard-Jones interaction between water molecules and nonstraight nanostructures. Our work offers an additional freedom to design high-flux nanochannels by choosing nonstraight nanostructures and provides an insight into water flow across biological water nanochannels, which are often nonstraight since they are composed of integral membrane proteins.

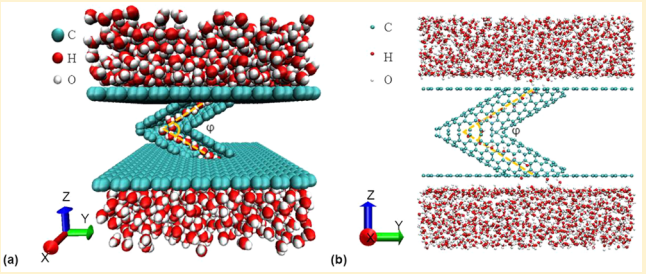

1. INTRODUCTION

Water molecules transporting across cell membranes play a strictly utilitarian role in biological activities,[1−9] and the understanding of this process involves some physical properties, for example, the protein−water coupling, temperature, and osmotic pressure.[3,9] Inspired by this extraordinary biological process, a lot of nanomachines and nanodevices have been invented, such as nanofiltration[10] and drug delivery.[11] Similar synthetic nanotubes have extended to applications of seawater desalination[12,13] and water purification.[14,15] Amazingly, the transport of water across nanochannels was found to be faster than the result of the "no-slip" hydrodynamic flow predicted from the Hagen−Poiseuille equation.[16,17] Moreover, water in carbon nanotubes is often compared with that inside biological nanochannels, the phenomenon of which is similar.[18−24] Such carbon nanotubes usually serve as a model system to mimic the function of biological structures and explore some basic behaviors of biological water nanochannels.[22−26]

It was also found that the capability of water permeation profoundly depends on the external conditions of the nanochannel systems. Accordingly, many external conditions (for example, mechanical forces, pressure gradient, or electric fields/charges) have been examined and investigated in researches of the transportation of water molecules through nanochannels which were often straight.[27−37]

In practice, nonstraight nanochannels are indispensable as well.[38] For example, Murata et al. reported that biological water nanochannels are generally nonstraight as a result of natural selection.[39] Falvo et al. showed that carbon nanotubes could be bent repeatedly up to large angles by using the tip of an atomic force microscope.[40] Iijima et al. found that at a critical bending angle a single V-shaped kink initiated when the carbon nanotube is subjected to compression.[41] Wang et al.[42] experimentally realized carbon nanorings from carbon nanotubes by using a Pickering emulsion-based process.[43] By arc discharge,[44] laser ablations,[45] and electric field methods,[46] the formations of L-junction, Y-junction, T-junction, and zigzag morphology carbon nanotubes were also reported.[46,47] Compared with nanotubes of perfectly straight geometry, such nonstraight nanochannels have been found that they can significantly alter electronic and thermal properties of carbon nanotubes.[48−51] However, how the nonstraight nanochannels affect water permeation has rarely been discussed. This might be due to the macroscopic scenario: when a nonstraight channel and a straight one are identical in the amount of inner surface area and volume, the numbers of average flow inside these two channels are equal under the same circumstances. A few researches involving nonstraight nanochannels[38,42,48−55] inspire us to investigate the effect of nonstraight carbon nanotubes on the transportation of single-file water molecules. In this work, we will show that this macroscopic scenario breaks down at the nanoscale of our interest.

2. METHODS

We followed Han et al.'s experimental observation (Figure 1a of ref 38) and designed a nonstraight single-walled carbon nanotube (SWCNT) for the simulations (see Figure 1a). In Figure 1a, an uncapped (10,0) nonstraight SWCNT with

Received: November 10, 2014
Revised: December 17, 2014
Published: January 6, 2015

DOI: 10.1021/jp511262w
J. Phys. Chem. B 2015, 119, 1496−1502

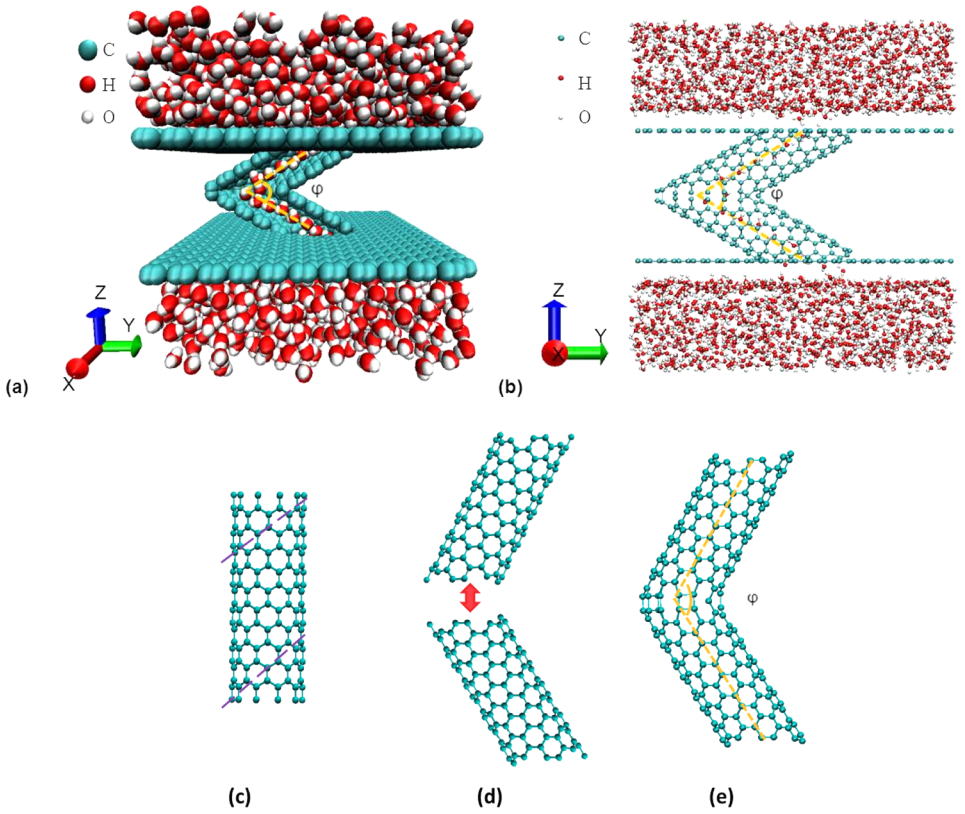

Figure 1. (a) A perspective view of the simulation system with a nonstraight SWCNT embedded between two parallel graphite sheets. The bent corner in the SWCNT is denoted by an angle of φ. We show the inner part of the SWCNT by removing some carbon atoms; the orange dashed line indicates the central path across the SWCNT, whose length is λ. More details can be found in the main text. (b) An orthographic projection of the model SWCNT with $\varphi = 60°$. (c)−(e) show the construction of a nonstraight carbon nanotube: (c) cut a (10,0) carbon nanotube in its top and bottom along the purple dashed lines, (d) join two cut nanotubes together, and (e) then get a bending nanotube with the bending angle φ.

diameter 0.777 nm is embedded between two parallel graphite sheets. There are reservoirs outside the two graphite sheets with no water existing between them except the space inside the nanotubes. The SWCNT has a bending angle of φ in its center portion. We have prepared 13 systems with bending angles φ = 35°, 40°, 45°, 52.5°, 60°, 75°, 90°, 105°, 120°, 135°, 150°, 165°, and 180° (which represents the case of a straight SWCNT). All the SWCNTs with different φ are set to possess the same central path, λ = 3.8 nm. The construction of a nonstraight nanotube is shown in Figure 1c−e. To construct these nonstraight SWCNTs, we connected two straight SWCNTs together with some topological defects such as carbon rings in the shape of irregular triangle, quadrilateral, pentagon, hexagon, heptagon, or even octagon.[38,53] For instance, Figure 1b shows the construction of a model SWCNT with φ = 60°: two straight (10,0) SWCNTs are connected by appropriately adding extra carbon rings shaped with triangle, quadrilateral, and pentagon in the position of the junction. Meanwhile, the total number of water molecules was set to be 1824 for each system whose water number density (namely, the number of water molecules per volume) was fixed in our simulations.

Our simulations were performed by using the GROMACS package,[56] a molecular dynamics package based on the Newtonian equations, and the TIP3P water model and Berendsen thermostat.[57,58] The carbon atoms here identified as uncharged particles were frozen, since the real motion of carbon atoms does not influence the qualitative results we have obtained. All atoms engaged in this research obey the Lennard-Jones (LJ) interaction, $V_{LJ} = 4\varepsilon[(\sigma/r)^{12} - (\sigma/r)^{6}]$, where ε is the depth of potential well and σ is the cross section of particles. These parameters adopted in our simulations come from ref 22. The periodic boundaries were set in the simulation boxes with dimensions (L_X, L_Y, L_Z), where L_X = 4.69 nm, L_Y = 4.69 nm, and L_Z = 4.56−6.90 nm. While setting the cutoff to be 1 nm, we performed the simulations in the canonical (NVT) ensemble at 300 K with time step 2 fs. Each system was carried out for 85 ns: the first 10 ns was seen as time for balance; the last 75 ns was used for statistical analysis. Without any external pressure difference, the water flow passed from either mouth of a nanotube because the Brownian motion, the effect of thermal fluctuation, was pushing it.

3. RESULTS AND DISCUSSION

Figure 2 shows the rate of transfer of water molecules across the SWCNTs with different bending angles, φ. The smaller the φ is, the more heavily a nanotube is deformed. φ of a straight nanotube is 180°. The rate of transfer here is defined as the sum of the numbers of water molecules, which had passed through the whole SWCNT from one mouth to another, per nanosecond. Obviously with the decay of φ, the rate of transfer increases. For the nanotube with φ = 35°, the maximum bending angle in this work, the result of rate of transform is 9.1 ns^{-1}, whereas the result of the straight nanotube with φ = 180° is 2.6 ns^{-1}. So the enhancement ratio between the two tubes is 3.5. As φ decreases from 60° to 35°, the number of the rate of transfer raises remarkably. However, when φ varies from 180° to 60°, the rate of transfer does not change significantly but

DOI: 10.1021/jp511262w
J. Phys. Chem. B 2015, 119, 1496−1502

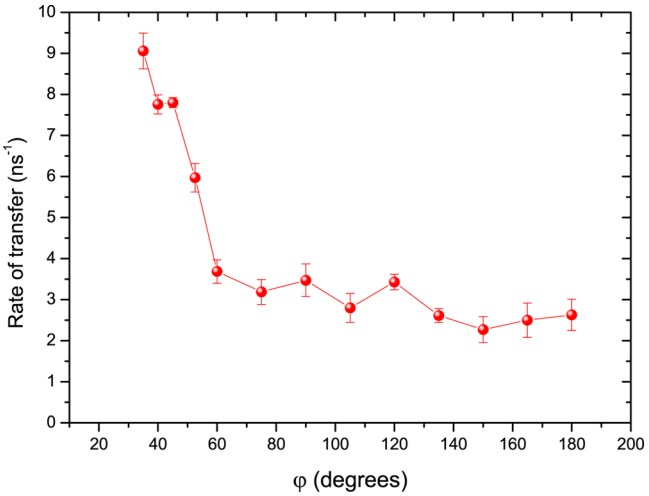

Figure 2. Rate of transfer of water molecules through SWCNTs with different φ = 35°, 40°, 45°, 52.5°, 60°, 75°, 90°, 105°, 120°, 135°, 150°, 165°, and 180°. Here φ = 180° denotes the straight SWCNT. The line is a guide for the eye; each symbol is accompanied by an error bar. Here we have divided the data of each system from 15 to 85 ns by seven intervals and calculated the means of the rate of transfer for the seven groups of data to get the error bars. Parameter: λ = 3.8 nm.

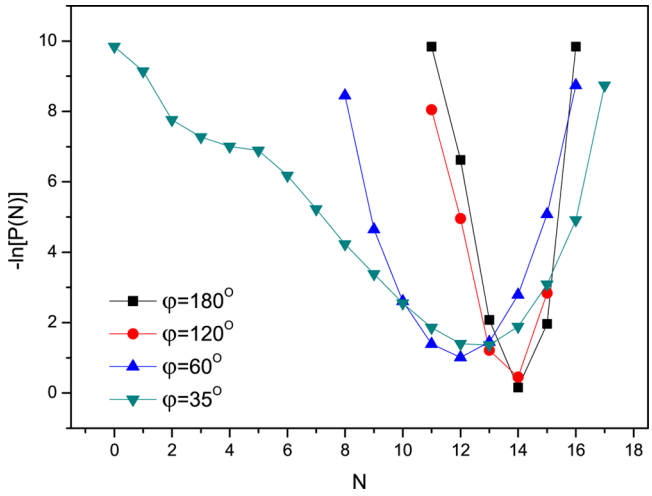

Figure 3. Free energy of occupancy fluctuations, $F(N) = -\ln[P(N)]/\beta$, for the four typical SWCNTs with φ = 35°, 60°, 120°, and 180°. Here $P(N)$ is the probability of finding N water molecules inside the SWCNT, and $\beta = (k_BT)^{-1}$, where k_B is the Boltzmann constant and T is the temperature. The lines are a guide for the eye. Parameter: λ = 3.8 nm.

only slightly increases according to the overall trend. These results indicate that water molecules inside a slightly distorted SWCNTs (i.e., φ > 60°) behave as they do in a straight nanotube whose φ = 180°. On the other hand, we have got a similar result from the simulation of a series of systems whose SWCNTs were bent in the same way but had the mouth opening area equal to the straight one. In these simulations, the enhance ratio between the 35° nanotube and the straight one is 3.01.

To get a full appreciation of what happened in nonstraight nanotubes, especially in the heavily bending ones (φ < 60°), we turn first to the calculation of free energy of occupancy fluctuations[22] for four typical nanotubes with φ = 35°, 60°, 120°, and 180° in Figure 3. We got this result by $F(N) = -\ln[P(N)]/\beta$, where $P(N)$ is the probability of finding N water molecules inside the SWCNT, $\beta = (k_BT)^{-1}$, k_B is the Boltzmann constant, and T is the temperature. The water occupancy profile of the straight SWCNT (φ = 180°) shows an approximate Gaussian distribution, which coincides with the previous studies.[22,59] N = 14 is the minimum of the straight case. For the nanotube with φ = 120°, the profile resembles the result of the straight one in shape and minimum position. In both cases, a single file of water was observed inside the nanotube. For the nanotubes with φ = 35° and 60°, however, the free energy profiles drastically deviate from the Gaussian distribution, and the minimum positions are N = 13 and 12, respectively. Apparently, water molecules in the φ = 35° naontube own more occupancy states than those in the other nanotubes in our simulations. The fluctuation of water number inside the nanotube multiplies considerably with the existence of the bent structure.

We have also plotted the Lennard-Jones potential of average interaction between one water molecule and a variety of nanotubes with φ = 35°, 60°, 90°, 120°, 150°, and 180°. The average LJ potential, shown in Figure 4a, is sensitive to bending angle φ. When a water molecule stays inside a nanotube with a larger φ, it is affected more by the carbons of the nanotube and the average LJ potential is lower. Although water molecules are more likely to enter a nanotube with lower LJ potential due to the stability from the lower energy state, the corresponding stronger water−nanotube restriction keeps these water molecules from escaping the tube, so that the water transportation is limited. Figure 4b shows the LJ potentials along the central path of the SWCNT between one water molecule and the SWCNT with φ = 35°, 60°, 120°, and 180°. Like the average value, the minimum values of LJ potential for the nonstraight nanotubes also larger than that of the straight tube. Compared with the profile of the straight nanotube, the LJ potential profile of the massively distorted nanotube (e.g., the nanotubes with φ = 35° or 60°) undulates greatly. In the vicinity of the center of the nanotubes with φ = 35°, in particular, the effect on a water molecule imposed by the carbon atoms rises up or falls down sharply when the molecule is going through the nanotube. Additionally, we calculated the LJ potential without giving consideration to the role played by the details of the defects in the nonstraight SWCNT at its middle point, where the two straight SWCNTs meet. The potential difference caused by the number of carbon atoms near the middle point varies negligibly according to different possible defects which could construct different details in the curvature of the nanotube.

Furthermore, the structure of bending nanotubes has significantly affected the water motion states especially in the center part of the tubes. Figure 5 illustrates two different situations when the water is inside two types of nanotubes: the space in the (10,0) nanotube allows only a single file of water molecules (Figure 5a), while there is enough space to accommodate a small rolling water cluster in the center part of a heavily bending nanotube (Figure 5b). To some extent, the bending structure warps the space where water molecules transit. The function of the nonstraight tube seems not to simply fold the motion paths of water but to make some part of water's paths overlapped and to locally create a bulklike circumstance. Enhanced water translocation involving water cluster inside the SWCNT was also observed in the work of Meng et al.[60] To quantify how water molecules arrange in the nanotubes, we have contrasted the pair correlation function for

DOI: 10.1021/jp511262w
J. Phys. Chem. B 2015, 119, 1496−1502

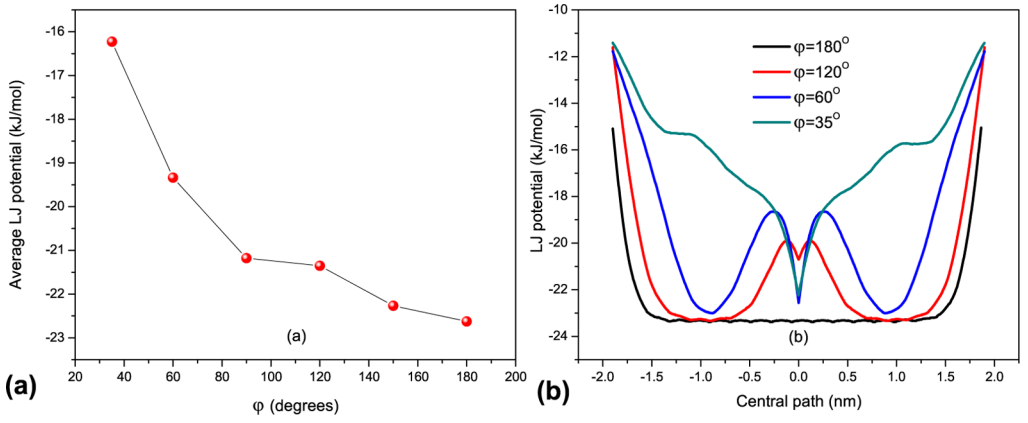

Figure 4. (a) Profile of average Lennard-Jones potentials between one water molecule and the SWCNT with φ = 35°, 60°, 90°, 120°, 150°, and 180°. (b) Profile of Lennard-Jones potentials along the central path of the SWCNT between one water molecule and the SWCNT with φ = 35°, 60°, 120°, and 180°. Parameter: λ = 3.8 nm.

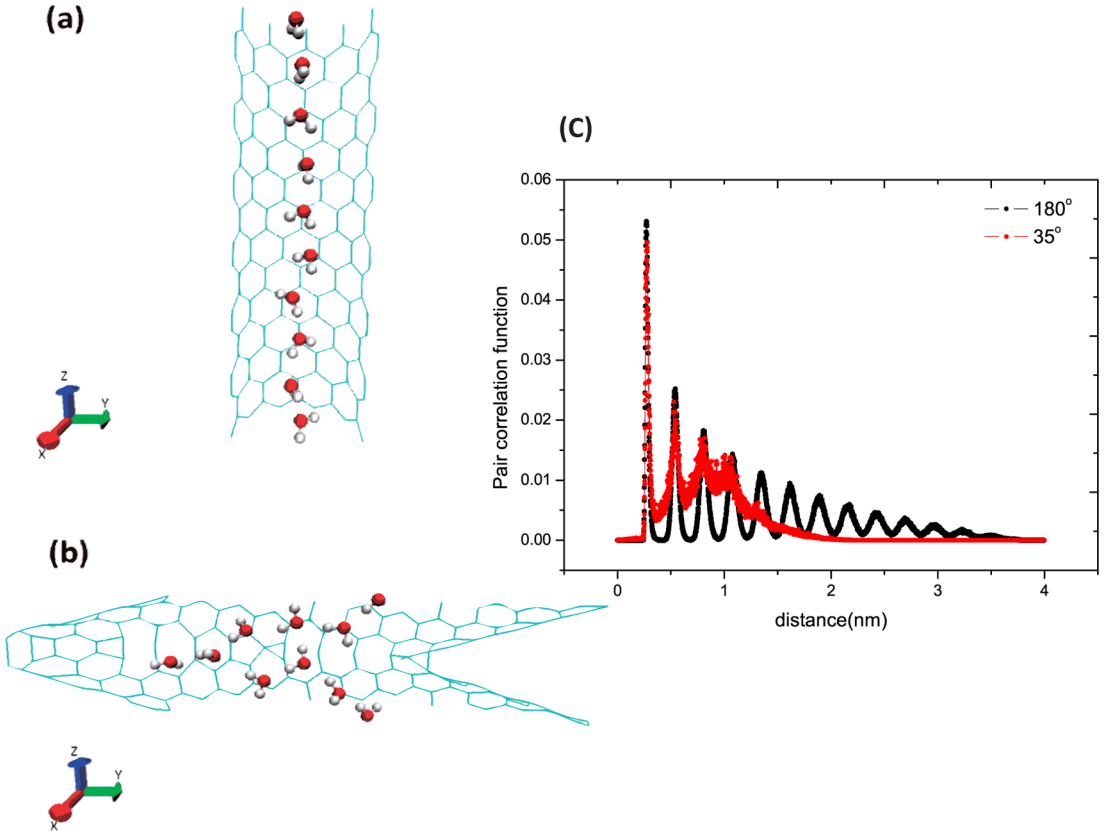

Figure 5. (a) Water molecules in the straight nanotube where the angle φ = 180°, namely the straight nanotube. (b) Water molecules in the nonstraight nanotube with the bending angle φ = 35°. (c) Pair correlation function $(1/N)\sum_{i=1}^{N}\sum_{j=1,j\neq1}^{N}\langle\delta(\vec{r}-\vec{r}_{ij})\rangle$ for the water molecules inside the nanotubes with nanotubes bending angle φ = 35° and 180°, where N is the number of water molecules inside a nanotube and $\vec{r}_{ij}$ is the vector between the coordinates of two oxygen atoms in water.

the water inside nanotube with angle φ = 35° and 180° in Figure 5c. The pair correlation function was calculated by the method from Mukherjee et al.,[61] $(1/N)\sum_{i=1}^{N}\sum_{j=1,j\neq1}^{N}\langle\delta(\vec{r}-\vec{r}_{ij})\rangle$ is taken as pair correlation function here, where N is the number of water molecules inside a nanotube and $\vec{r}_{ij}$ is the vector between the coordinates of two oxygen atoms in water. A similar pair correlation function profile, which reveals "solidlike" ordering of water, has been obtained in Mukherjee's work[61] when the bending angle is 180° (the straight nanotube). The distinct peaks in profiles of straight and nonstraight tubes appear in the same position, for the potential parameters among water molecules are identical in our simulations. Despite the same positions of peaks of the two profiles, the peaks of the nonstraight nanotube with the bending angle φ = 35° relax more slowly than those in the straight CNT, coinciding with the fact that water molecules tend to concentrate together more densely near the center of the nanotube. It is apparent that the large deformation makes the water arrangement in the nanotube close to bulk water in contrast with a single chain in the straight nanotube. Additionally, because the flow

DOI: 10.1021/jp511262w
J. Phys. Chem. B 2015, 119, 1496−1502

enhancement results from the more free motion of water molecules near the center of the nonstraight nanotubes, the large enhancement of water flow will be unaffected in the presence of a pressure difference across the system.

In Figure 6, we present the profiles of the potential of mean force along the Z-axis by using $-k_BT \ln[P(N)]$, where P is the average probability of water molecules along the Z-axis, k_BT is the Boltzmann constant, and T is the thermodynamic temperature. Two sides of each profile come from bulk region of the reservoirs, and central region is the higher energy barrier due to the impediment of the carbon nanotube. In the case of straight nanotube with $\varphi = 180°$ and slightly bending nanotube with $\varphi = 120°$, the free energy barriers are higher and almost flat. The potential energy surface of the straight case is in good accordance with the profile by Beu.[62] For the heavily bending nanotubes with $\varphi = 35°$ and 60°, there exits appreciable shaking in the center of part free energy barrier which are still lower than that of the straight case and slightly bending tube. Water molecules have to surmount the potential barriers, which are lower in smaller bending angle nanotubes, to go through the nanotube from one mouth to another. Since the bending structure provides more space for water to break the single file in the center part of the tube (e.g., nanotube with $\varphi = 35°$ (Figure 5b)), water molecules congregate together there and work themselves into reducing free energy barriers. In this way, the lower free energy barrier from the stronger interaction among water improves the transfer rate when water molecules go through the heavily bending carbon nanotubes with small φ.

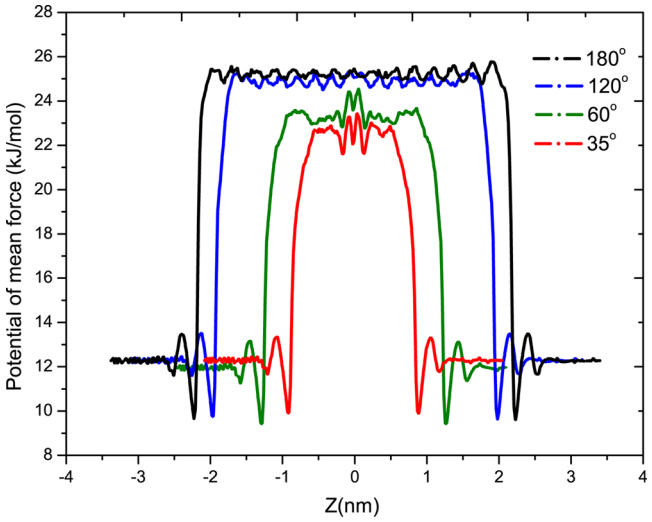

Figure 6. Potential of mean force (PMF) profiles along the Z-axis in systems with nanotubes bendng angle $\varphi = 35°$, 60°, 120°, and 180°, and the potential of mean force was calculated by $-k_BT \ln[P(N)]$, where P is the average probability of water molecules along the Z direction, k_BT is the Boltzmann constant, and T is the temperature.

4. CONCLUSION

In summary, we have shown that the macroscopic scenario mentioned at the beginning of this work fails at the nanoscale: significantly nonstraight nanochannels produce less friction to transfer single-file water molecules than the straight nanochannel. In particular, the nonstraight nanostructure can raise the rate of transfer of water molecules across the SWCNT maximally by 3.5 times in our simulations. This increment results from the fact that nonstraight nanostructure holds the water cluster which causes the higher fluctuation and lower free energy barrier. In practice, a carbon nanotube can be either a metal or a semiconductor,[63,64] but this does not affect the current impact of the nonstraight structure. Similarly, our results will not change if someone replaces the SWCNT with a multiwalled carbon nanotube. This is because the spatial structure of the water molecules located in a multiwalled carbon nanotube would keep unchanged, and the calculation of the LJ potentials holds as well. On the same footing, if one considers a nanochannel, which is beyond carbon nanotubes, our results should be valid as well. Yet the enhancement effect will become ignorable if the diameter of the nanotube increases because the effect of breaking the single-chain water diminishes in the nonstraight tubes with large diameter. The extreme example is a macrosize nonstraight tube, in which the water flow rate is equal to that of the straight tube if the two tubes have the same values of the diameter and inner volume. The present study might enlighten the nanomechanical engineering for high-efficiency water flow. On the other hand, this work could inspire the research about water movement across nanochannels in biological membranes; such nanochannels are often nonstraight because they are constructed by soft matter like proteins.

AUTHOR INFORMATION

Corresponding Author

*E-mail: jphuang@fudan.edu.cn (J.P.H.).

Notes

The authors declare no competing financial interest.

ACKNOWLEDGMENTS

We are grateful to Dr. Y. Wang of Zhejiang Agriculture and Forestry University for fruitful discussions. We acknowledge the financial support by the National Natural Science Foundation of China under Grant 11222544, by the Fok Ying Tung Education Foundation under Grant 131008, by the Program for New Century Excellent Talents in University (NCET-12-0121), and by the CNKBRSF under Grant 2011CB922004. The computational resources utilized in this research were provided by Shanghai Supercomputer Center.

REFERENCES

(1) Kaszuba, K.; Rog, T.; Bryl, K.; Vattulainen, I.; Karttunen, M. Molecular dynamics simulations reveal fundamental role of water as factor determining affinity of binding of beta-blocker nebivolol to beta(2)-adrenergic receptor. *J. Phys. Chem. B* **2010**, *114*, 8374−8386.

(2) de Groot, B. L.; Grubmuller, H. Water permeation across biological membranes: Mechanism and dynamics of aquaporin-1 and GlpF. *Science* **2001**, *294*, 2353−2357.

(3) Wood, K.; Plazanet, M.; Gable, F.; Kessler, B.; Oesterhel, D.; Tobias, D. J.; Zaccai, G.; Weik, M. Coupling of protein and hydration-water dynamics in biological membranes. *Proc. Natl. Acad. Sci. U. S. A.* **2007**, *104*, 18049−18054.

(4) Gong, X.; Li, J.; Zhang, H.; Wan, R.; Lu, H.; Wang, S.; Fang, H. P. Enhancement of water permeation across a nanochannel by the structure outside the channel. *Phys. Rev. Lett.* **2008**, *101*, 257801.

(5) Xu, B. X.; Li, Y. B.; Park, T.; Chen, X. Effect of wall roughness on fluid transport resistance in nanopores. *J. Chem. Phys.* **2011**, *135*, 144703.

(6) Li, X. Y.; Shi, Y. C.; Yang, Y. L.; Du, H. L.; Zhou, R. H.; Zhao, Y. L. How does water-nanotube interaction influence water flow through the nanochannel? *J. Chem. Phys.* **2012**, *136*, 175101.

DOI: 10.1021/jp511262w
J. Phys. Chem. B 2015, 119, 1496−1502

(7) Thomas, J. A.; McGaughey, A. J. H. Water flow in carbon nanotubes: Transition to subcontinuum transport. *Phys. Rev. Lett.* **2009**, *102*, 184502.
(8) Hashido, M.; Kidera, A.; Ikeguchi, M. Water transport in aquaporins: osmotic permeability matrix analysis of molecular dynamics simulations. *Biophys. J.* **2007**, *93*, 373−385.
(9) Borgnia, M.; Nielsen, S.; Engel, A.; Agre, P. Cellular and molecular biology of the aquaporin water channels. *Annu. Rev. Biochem.* **1999**, *68*, 425−458.
(10) Vlassiouk, I.; Smirnov, S.; Siwy, Z. Ionic selectivity of single nanochannels. *Nano Lett.* **2008**, *8*, 1978−1985.
(11) Panczyk, T.; Warzocha, T. P.; Camp, P. J. A magnetically controlled molecular nanocontainer as a drug delivery system: The effects of carbon nanotube and magnetic nanoparticle parameters from Monte Carlo simulations. *J. Phys. Chem. C* **2010**, *114*, 21299−21308.
(12) Service, R. F. Desalination freshens up. *Science* **2006**, *313*, 1088−1090.
(13) Corry, B. Designing carbon nanotube membranes for efficient water desalination. *J. Phys. Chem. B* **2008**, *112*, 1427−1434.
(14) Nasrabadi, A. T.; Foroutan, M. Ion-separation and water-purification using single-walled carbon nanotube electrodes. *Desalination* **2001**, *227*, 236−243.
(15) Wang, X. B.; Jin, L.; Xu, W. Z.; Cao, T.; Song, X. J.; Cheng, S. L. Preparation of carbon microstructures by thermal treatment of thermosetting/thermoplastic polymers and their application in water purification. *Micro Nano Lett.* **2012**, *7*, 918−922.
(16) Majumder, M.; Chopra, N.; Hinds, B. J. Mass transport through carbon nanotube membranes in three different regimes: Ionic diffusion and gas and liquid flow. *ACS Nano* **2011**, *5*, 3867−3877.
(17) Holt, J. K.; Park, H. G.; Wang, Y.; Stadermann, M.; Artyukhin, A. B.; Grigoropoulos, C. P.; Noy, A.; Bakajin, O. Fast mass transport through sub-2-nanometer carbon nanotubes. *Science* **2006**, *312*, 1034−1037.
(18) Cambre, S.; Schoeters, B.; Luyckx, S.; Goovaerts, E.; Wenseleers, W. Experimental observation of single-file water filling of thin single-wall carbon nanotubes down to chiral index (5,3). *Phys. Rev. Lett.* **2010**, *104*, 207401.
(19) Wang, Y.; Zhao, Y. J.; Huang, J. P. Giant pumping of single-file water molecules in a carbon nanotube. *J. Phys. Chem. B* **2011**, *115*, 13275−13279.
(20) Lu, H.; Li, J.; Gong, X.; Wan, R.; Zeng, L.; Fang, H. P. Water permeation and wavelike density distributions inside narrow nanochannels. *Phys. Rev. B* **2008**, 174115.
(21) Su, J. Y.; Guo, H. X. Control of unidirectional transport of single-file water molecules through carbon nanotubes in an electric field. *ACS Nano* **2011**, *5*, 351−359.
(22) Hummer, G.; Rasaiah, J. C.; Noworyta, J. P. Water conduction through the hydrophobic channel of a carbon nanotube. *Nature* **2001**, *414*, 188−190.
(23) Meng, X. W.; Wang, Y.; Zhao, Y. J.; Huang, J. P. Gating of a water nanochannel driven by dipolar molecules. *J. Phys. Chem. B* **2011**, *115*, 4768−4773.
(24) Li, J. Y.; Gong, X. J.; Lu, H. J.; Li, D.; Zhou, R. H. Electrostatic gating of a nanometer water channel. *Proc. Natl. Acad. Sci. U. S. A.* **2007**, *104*, 3687−3692.
(25) Gong, X. J.; Li, J. Y.; Lu, H. J.; Wan, R. Z.; Li, J. C.; Hu, J.; Fang, H. P. A charge-driven molecular water pump. *Nat. Nanotechnol.* **2007**, *2*, 709−712.
(26) Wan, R. Z.; Li, J. Y.; Lu, H. J.; Fang, H. P. Controllable water channel gating of nanometer dimensions. *J. Am. Chem. Soc.* **2005**, *127*, 7166−7170.
(27) Zhou, X. Y.; Wu, F. M.; Kou, J. L.; Nie, X. C.; Liu, Y.; Lu, H. J. Vibrating-charge-driven water pump controlled by the deformation of the carbon nanotube. *J. Phys. Chem. B* **2013**, *117*, 11681−11686.
(28) Chaudhury, M. K.; Whitesides, G. M. How to make water run uphill. *Science* **1992**, *256*, 1539−1541.
(29) Linke, H.; Aleman, B. J.; Melling, L. D.; Taormina, M. J.; Francis, M. J.; Dow-Hygelund, C. C.; Narayanan, V.; Taylor, R. P.; Stout, A. Self-propelled Leidenfrost droplets. *Phys. Rev. Lett.* **2006**, *96*, 154502.
(30) Qiao, R.; Aluru, N. R. Atypical dependence of electroosmotic transport on surface charge in a single-wall carbon nanotube. *Nano Lett.* **2003**, *3*, 1013−1017.
(31) Detcheverry, F.; Bocquet, L. Thermal fluctuations in nanofluidic transport. *Phys. Rev. Lett.* **2012**, *109*, 024501.
(32) Falk, K.; Sedlmeier, F.; Joly, L.; Netz, R. R.; Bocquet, L. Molecular origin of fast water transport in carbon nanotube membranes: Superlubricity versus curvature dependent friction. *Nano Lett.* **2010**, *10*, 4067−4073.
(33) Kalra, A.; Garde, S.; Hummer, G. Osmotic water transport through carbon nanotube membranes. *Proc. Natl. Acad. Sci. U. S. A.* **2003**, *100*, 10175−10180.
(34) Pascal, T. A.; Goddard, W. A.; Jung, Y. S. Entropy and the driving force for the filling of carbon nanotubes with water. *Proc. Natl. Acad. Sci. U. S. A.* **2011**, *108*, 11794−11798.
(35) Mikami, F.; Matsuda, K.; Kataura, H.; Maniwa, Y. Dielectric properties of water inside single-walled carbon nanotubes. *ACS Nano* **2009**, *3*, 1279−1287.
(36) Agrawal, B. K.; Singh, V.; Pathak, A.; Srivastava, R. Ab initio study of H_2O and water-chain-induced properties of carbon nanotubes. *Phys. Rev. B* **2007**, *75*, 195421.
(37) Liu, Y. C.; Wang, Q. Transport behavior of water confined in carbon nanotubes. *Phys. Rev. B* **2005**, *72*, 085420.
(38) Han, J.; Anantram, M. P.; Jaffe, R. L.; Kong, J.; Dai, H. Observation and modeling of single-wall carbon nanotube bend junctions. *Phys. Rev. B* **1998**, *57*, 14983−14989.
(39) Murata, K.; Mitsuoka, K.; Hirai, T.; Walz, T.; Agre, P.; Heymann, J. B.; Engel, A.; Fujiyoshi, Y. Structural determinants of water permeation through aquaporin-1. *Nature* **2000**, *407*, 599−605.
(40) Falvo, M. R.; Clary, G. J.; Taylor, R. M.; Chi, V.; Brooks, F. P.; Washburn, S.; Superfine, R. Bending and buckling of carbon nanotubes under large strain. *Nature* **1997**, *389*, 582−584.
(41) Iijima, S.; Brabec, C.; Maiti, A.; Bernholc, J. Structural flexibility of carbon nanotubes. *J. Chem. Phys.* **1996**, *104*, 2089−2092.
(42) Wang, W.; Laird, E. D.; Gogotsi, Y.; Li, C. Y. Bending single-walled carbon nanotubes into nanorings using a Pickering emulsion-based process. *Carbon* **2012**, *50*, 1769−1775.
(43) Chen, G.; Tan, P.; Chen, S.; Huang, J. P.; Wen, W.; Xu, L. Coalescence of pickering emulsion droplets induced by an electric field. *Phys. Rev. Lett.* **2013**, *110*, 064502.
(44) Iijima, S.; Ichihashi, T. Single-shell carbon nanotubes of 1-nm diameter. *Nature* **1993**, *363*, 603−605.
(45) Liu, J.; Dai, H.; Hafner, J. H.; Colbert, D. T.; Tans, S. J.; Dekker, C.; Smalley, R. E. Fullerene 'crop circles'. *Nature* **1997**, *385*, 780−781.
(46) AuBuchon, J. F.; Chen, L. H.; Gapin, A. I.; Kim, D. W.; Daraio, C.; Jin, S. H. Multiple sharp bendings of carbon nanotubes during growth to produce zigzag morphology. *Nano Lett.* **2004**, *4*, 1781−1784.
(47) Zhou, D.; Seraphin, S. Complex branching phenomena in the growth of carbon nanotubes. *Chem. Phys. Lett.* **1995**, *238*, 286−289.
(48) Ruoff, R. S.; Tersoff, J.; Lorents, D. C.; Subramoncy, S.; Chan, B. Radial deformation of carbon nanotubes by van-der-Waals forces. *Nature* **1993**, *364*, 514−516.
(49) Kane, C. L.; Mele, E. J. Size, shape, and low energy electronic structure of carbon nanotubes. *Phys. Rev. Lett.* **1997**, *78*, 1932−1935.
(50) Chibotaru, L. F.; Bovin, S. A.; Ceulemans, A. Bend-induced insulating gap in carbon nanotubes. *Phys. Rev. B* **2002**, *66*, 161401.
(51) Huang, Z. X.; Tang, Z. A.; Yu, J.; Bai, S. Y. Temperature-dependent thermal conductivity of bent carbon nanotubes by molecular dynamics simulation. *J. Appl. Phys.* **2011**, *109*, 104316.
(52) Li, X.; Yang, W.; Liu, B. Bending induced rippling and twisting of multiwalled carbon nanotubes. *Phys. Rev. Lett.* **2007**, *98*, 205502.
(53) Meunier, V.; Henrard, L.; Lambin, P. Energetics of bent carbon nanotubes. *Phys. Rev. B* **1998**, *57*, 2586−2591.
(54) Teich, D.; Fthenakis, Z. G.; Seifert, G.; Tomanek, D. Nanomechanical energy storage in twisted nanotube ropes. *Phys. Rev. Lett.* **2012**, *109*, 255501.

DOI: 10.1021/jp511262w
J. Phys. Chem. B 2015, 119, 1496−1502

(55) Mazzoni, M. S. C.; Chacham, H. Atomic restructuring and localized electron states in a bent carbon nanotube: A first-principles study. *Phys. Rev. B* **2000**, *61*, 7312−7315.
(56) http://www.gromacs.org.
(57) Jorgensen, W. L.; Chandrasekha, J.; Madura, J. D.; Impey, R. W.; Klein, M. L. Comparison of simple potential functions for simulating liquid water. *J. Chem. Phys.* **1983**, *79*, 926−935.
(58) Berendsen, H. J. C.; Postma, J. P. M.; van Gunsteren, W. F.; DiNola, A.; Haak, J. R. Molecular-dynamics with coupling to an external bath. *J. Chem. Phys.* **1984**, *81*, 3684−3690.
(59) Wan, R.; Li, G.; Lu, H.; Fang, H. Controllable water channel gating of nanometer dimensions. *J. Am. Chem. Soc.* **2005**, *127*, 7166−7170.
(60) Meng, X. W.; Huang, J. P. Enhanced permeation of single-file water molecules across a noncylindrical nanochannel. *Phys. Rev. E* **2013**, *88*, 014104.
(61) Mukherjee, B.; Maiti, P. K.; Dasgupta, C.; Sood, A. K. Strong correlations and Fickian water diffusion in narrow carbon nanotubes. *J. Chem. Phys.* **2007**, *126*, 124704.
(62) Beu, T. A. Molecular dynamics simulations of ion transport through carbon nanotubes. I. Influence of geometry, ion specificity, and many-body interactions. *J. Chem. Phys.* **2010**, *132*, 164513.
(63) Dresselhaus, M. S.; Dresselhaus, G.; Eklund, P. *Science of Fullerenes and Carbon Nanotubes*; Academic: New York, 1996.
(64) Kozinsky, B.; Marzari, N. Static dielectric properties of carbon nanotubes from first principles. *Phys. Rev. Lett.* **2006**, *96*, 166801.

DOI: 10.1021/jp511262w
J. Phys. Chem. B 2015, 119, 1496−1502